

Article

Distributed Fault Diagnosis via Iterative Learning for Partial Differential Multi-Agent Systems with Actuators

Cun Wang ^{1,2} , Zupeng Zhou ^{1,*} and Jingjing Wang ^{2,*}

¹ School of Mechanical and Electrical Engineering, Guilin University of Electronic Technology, Guilin 541004, China; gxutwc@163.com

² School of Vocational and Technical Education, Guangxi Science & Technology Normal University, Laibin 546199, China

* Correspondence: zhouzupeng@guet.edu.cn (Z.Z.); wangjingjing@gxstnu.edu.cn (J.W.)

Abstract: Component failures can lead to performance degradation or even failure in multi-agent systems, thus necessitating the development of fault diagnosis methods. Addressing the distributed fault diagnosis problem in a class of partial differential multi-agent systems with actuators, a fault estimator is designed under the introduction of virtual faults to the agents. A P-type iterative learning control protocol is formulated based on the residual signals, aiming to adjust the introduced virtual faults. Through rigorous mathematical analysis utilizing contraction mapping and the Bellman–Gronwall lemma, sufficient conditions for the convergence of this protocol are derived. The results indicate that the learning protocol ensures the tracking of virtual faults to actual faults, thereby facilitating fault diagnosis for the systems. Finally, the effectiveness of the learning protocol is validated through numerical simulation.

Keywords: multi-agent systems; distributed fault diagnosis; partial differential equations; iterative learning control

MSC: 93A16; 93B70; 68T20



Citation: Wang, C.; Zhou, Z.; Wang, J. Distributed Fault Diagnosis via Iterative Learning for Partial Differential Multi-Agent Systems with Actuators. *Mathematics* **2024**, *12*, 955. <https://doi.org/10.3390/math12070955>

Academic Editor: Yolanda Vidal

Received: 20 February 2024

Revised: 12 March 2024

Accepted: 21 March 2024

Published: 23 March 2024



Copyright: © 2024 by the authors. Licensee MDPI, Basel, Switzerland. This article is an open access article distributed under the terms and conditions of the Creative Commons Attribution (CC BY) license (<https://creativecommons.org/licenses/by/4.0/>).

1. Introduction

In the past decade, research on multi-agent systems (MASs) has garnered widespread attention [1–6]. MASs consist of intelligent entities with sensing and execution capabilities, collaborating through network coupling to collectively solve problems, thereby enhancing the efficiency of problem solving [1,2]. Due to their advantages, MASs find extensive applications in collaborative research areas such as unmanned ground vehicles [3], unmanned boats [4], and drones [5]. A detailed survey of the application domains of MASs is conducted in [6].

The successful completion of complex tasks through cooperation in MASs is contingent upon the normal operation of each agent and the maintenance of regular communication connections between agents [7]. However, unlike the single intelligent system described by ordinary differential equations (ODEs) in [8–10], with an increase in the number of agents, the long-term operation of MASs becomes more susceptible to the influence of failures in practice [11]. Suppose that faults should be promptly diagnosed and addressed after occurrence, the distributed nature of MASs makes faults prone to propagating among their networks, leading to MAS paralysis and causing severe economic losses [12]. Consequently, considering the reliability and security of MASs in real-world scenarios, issues related to fault diagnosis have garnered widespread attention [13–17]. For instance, in [13], a sliding mode observer addressed the fault detection issue in MASs subject to disturbances. In [14], a distributed fault diagnosis approach for MASs was proposed based on a belief rule base. Furthermore, in [15], a novel iterative learning control scheme was developed to mitigate the impact of uncertainties and actuator failures in MASs. In contrast, the scheme relied on

estimating both the self-state and the neighboring states. Additional research reports on fault diagnosis in MASs can be found in references [16,17].

Iterative learning control (ILC) represents an effective intelligent control strategy for achieving the high-precision tracking of an unknown system with accurate models within a finite time interval [18]. It is particularly well suited to systems exhibiting repetitive cyclic tracking characteristics. ILC, initially proposed by Arimoto and others, is a significant branch of learning control [19,20]. The core idea of ILC involves utilizing the input–output data obtained from previous iterations, continuously refining the control input from the previous iteration, and achieving the complete tracking of the desired trajectory within a finite time interval [21,22]. Compared to some traditional control methods, ILC requires minimal prior knowledge and computations, making it suitable for straightforwardly handling dynamic systems with high uncertainty [23]. Consequently, ILC has been widely researched in both practical and theoretical analyses of MASs [24,25]. In recent years, ILC has made significant strides in system fault diagnosis [26–28]. For example, in [26], an investigation was conducted on iterative learning fault diagnosis for stochastic repeat systems with Brownian motion. In [27], a novel fault detection and estimation algorithm based on ILC was proposed to address the challenges of detecting and estimating faults in time-varying uncertain network systems. Subsequently, an effective data-driven ILC scheme was designed for a specific class of network systems with potential faults [28]. Thus, the objective of diagnosing system faults can be achieved by iteratively adjusting the introduced virtual faults through the residual signal using ILC methods. Unfortunately, as evident from the mentioned references [13–17,26–28], these studies primarily address fault diagnosis issues in the time domain for MASs.

Despite this, recent research has yielded novel findings on MASs described by ODEs [29–31], with ample consideration given to the temporal evolution of agent states. However, in the real world, the state of MASs is not only time-dependent but also spatially influenced, as observed in examples such as flexible robotic arms, the axial movement of motors, and spacecraft surfaces, as referenced in [32–35]. Consequently, in recent years, significant efforts have been dedicated to addressing the control issues of MASs modeled by partial differential equations (PDEs) [36–39]. In [36], considering the spatiotemporal dynamic evolution of agents, the partial differential MAS dynamic model was established through PDEs to describe this behavior. In [37], the consensus problem of a class of non-linear pulse partial MASs was addressed by applying ILC methods. Furthermore, [38] and [39] employed ILC schemes to solve the consensus control problem of discretized partial differential MASs, respectively. This indicates that ILC can effectively address the coordinated control issues of partial differential MASs. Compared to the previously mentioned ordinary differential MASs, partial differential MASs are more prone to faults due to the spatiotemporal complexity of their states. More preliminary research on the fault diagnosis problem in spatiotemporal partial differential MASs must be conducted, presenting an open and challenging field. In this context, developing reliable fault detection methods specifically tailored to partial differential MASs becomes a critical and urgent challenge hindering their advancement.

This study investigates the distributed fault diagnosis problem of a class of linear partial differential MASs with actuators using the ILC method. Firstly, a fault estimator is designed by introducing virtual faults to the agents. Secondly, a P-type ILC protocol is formulated based on the error between the actual systems' output and the fault estimator's (residual signal) output. After this control protocol is applied, the introduced virtual faults converge to the actual faults, achieving the goal of fault diagnosis for the partial differential MASs. Finally, the effectiveness of the learning protocol is validated through numerical simulation examples.

The main contributions of this work are summarized in the following key points:

- (1) Unlike the fault diagnosis for ordinary differential MASs discussed in [13–17], this work addresses the fault diagnosis problem for a class of partial differential MASs over

a continuous spatiotemporal period. The aim is to tackle the limitations hindering the in-depth development of partial differential MASs.

- (2) Based on the ILC method, a distributed P-type ILC protocol with high-precision tracking performance is constructed to address the fault diagnosis problem of partial differential MASs with actuators. This learning process exhibits strong resistance to disturbances compared to traditional observers.
- (3) The necessary and sufficient conditions for fault diagnosis in partial differential MASs are derived through the application of contraction mapping and the Bellman–Gronwall lemma. Despite the intricate spatiotemporal dynamics of the agents, this derivation further enriches the theoretical achievements in fault diagnosis for MASs.

The remaining sections of the article are organized as follows: In Section 2, fundamental knowledge will be provided, problem will be formulated under certain assumptions, and a description of the MASs is presented. Section 3 will focus on the design of a suitable fault estimator and ILC protocol. The analysis of the convergence conditions for estimating MAS faults will be presented in Section 4. Simulation results and conclusions will be provided in Sections 5 and 6, respectively.

2. Preliminaries and Problem Statement

2.1. Preliminaries

Algebraic graph theory is frequently employed to depict the communication relationships among agents in MASs. Let $\bar{G} = (\bar{V}, \bar{E}, \bar{A})$ describe the directed graph of the network consisting of N agents in the system. Here, $\bar{V} = \{\bar{v}_1, \bar{v}_2, \dots, \bar{v}_N\}$ is the set of nodes in graph \bar{G} , and $\bar{E} \subseteq \bar{V} \times \bar{V}$ is the set of its edges. Moreover, $\bar{e}_{j,i} \in \bar{E}$ implies that there is a communication link from node j to node i . $\bar{A} = [\bar{a}_{j,i}] \in \mathbb{R}^{N \times N}$ is the adjacency matrix, where $\bar{a}_{j,i} > 0 \Leftrightarrow \bar{e}_{j,i} \in \bar{E}$. Define $\bar{D} = \text{diag}(\bar{d}_1, \bar{d}_2, \dots, \bar{d}_N)$ as the degree matrix of graph \bar{G} , then the degree of node j is $\bar{d}_j = \sum_{i \in N_j} \bar{a}_{ji}$, where N_j is the set of neighbors for agent j . The Laplacian matrix of graph \bar{G} is $\bar{L} = \bar{D} - \bar{A}$. Additionally, \otimes is the Kronecker product, I_N is the identity matrix, and the transpose of matrix C is C^T .

Furthermore, for the n -dimensional vector $X = (x_1, x_2, \dots, x_n)^T$, its norm is defined as $\|X\| = \sqrt{\sum_{l=1}^n x_l^2}$, and the norm of the corresponding $n \times n$ -dimensional matrix A is $\|A\| = \sqrt{\lambda_{\max}(A^T A)}$, where $\lambda_{\max}(\cdot)$ denotes the maximum eigenvalue. Let $L^2(\Omega)$ be the function space consisting of all measurable functions satisfying $\|p\|_{L^2}^2 = \int_{\Omega} |p(s)|^2 ds < \infty$.

If $p_l(s) \in L^2(\Omega)$, $l = 1, 2, \dots, n$, then $P = (p_1, p_2, \dots, p_n) \in \mathbb{R}^n \cap L^2(\Omega)$ holds, and $\|P\|_{L^2} = \{\int_{\Omega} P^T(s)P(s)ds\}^{\frac{1}{2}}$. For a given positive constant λ , (L^2, λ) is defined as $\|P\|_{(L^2, \lambda)} = \sup_{0 \leq t \leq T} \{\|P(\cdot, t)\|_{L^2}^2 e^{-\lambda t}\}$.

The following lemma lays the foundation for the convergence analysis of the subsequent main results, and the lemma used is as follows:

Lemma 1. (Contraction mapping principle [40]). *For a non-negative real sequence p_k satisfying $p_{k+1} \leq \theta p_k + \omega_k$, where $0 \leq \theta < 1$ and $\lim_{k \rightarrow \infty} \omega_k = 0$, it holds that $\lim_{k \rightarrow \infty} p_k = 0$.*

Lemma 2 (Bellman–Gronwall Inequality [41]). *Assuming $r_1(t)$ and $r_2(t)$ are the real-valued continuous function in the interval $[0, T]$, and $\zeta_1 \geq 0$, if $r_1(t) \leq \zeta_3 + \int_0^t (\zeta_1 r_1(\tau) + \zeta_2 r_2(\tau)) d\tau$, then $r_1(t) \leq \zeta_3 e^{\zeta_1 t} + \int_0^t e^{\zeta_1(t-\tau)} \zeta_2 r_2(\tau) d\tau$.*

2.2. Problem Statement

Consider the parabolic partial differential MAS composed of N actuators that performs repeatable tasks. Among them, the dynamic model of the j -th agent actuator is as follows:

$$\begin{cases} \frac{\partial p_j(s,t)}{\partial t} = H\Delta p_j(s,t) + Ap_j(s,t) + Bu_j(s,t) + Ef_j(s,t), \\ y_j(s,t) = Cp_j(s,t) + Du_j(s,t) + Ff_j(s,t), \end{cases} \quad (1)$$

where $j = 1, 2, \dots, N$ denotes the label of the actuator agent, and $(s, t) \in \Omega \times [0, T]$, while Ω represents a smooth and bounded region. The state, input, and output of the actuator agent j are, respectively, denoted by $p_j(s, t) \in R^n$, $u_j(s, t) \in R^m$ and $y_j(s, t) \in R^p$. The matrix H is a positive and bounded diagonal matrix, specifically with $H = \text{diag}[h_1, h_2, \dots, h_n] \in R^{n \times n}$ and $0 < h_l < \infty$. The matrices $A \in R^{n \times n}$, $B, E \in R^{n \times m}$, $C \in R^{p \times n}$ and $D, F \in R^{p \times m}$ are all bounded matrices. $f_j(s, t) \in R^m$ represents the fault signal for actuator agent j , and Δ is the Laplace operator defined on the region Ω , i.e., $\Delta = \sum_{l=1}^p \frac{\partial^2}{\partial s_l^2}$. Meanwhile, the initial and boundary conditions for MAS (1) are as follows:

$$\sigma p_j(s, t) + \beta \frac{\partial p_j(s, t)}{\partial v} = 0, (s, t) \in \partial\Omega \times [0, T], \quad (2)$$

$$p_j(s, t) = \varphi_j(s), s \in \Omega, j \in \{1, 2, \dots, N\}, \quad (3)$$

where $\sigma = \text{diag}[\sigma_1, \sigma_2, \dots, \sigma_n], \sigma_l \geq 0$, $\beta = \text{diag}[\beta_1, \beta_2, \dots, \beta_n], \beta_l > 0$, and $\frac{\partial}{\partial v}$ represents the outward normal vector on the boundary $\partial\Omega$ of the region.

Building upon the strategies outlined in the literature above [15,26–28], which utilize the ILC scheme for system fault diagnosis, to diagnose faults in MAS (1), an appropriate ILC is designed to design a suitable fault estimator. Simultaneously, while ensuring the convergence of the designed learning protocol, the following assumptions need to be satisfied for the fault diagnosis of the actual output and fault estimation output of the MAS (1):

Assumption 1. The communication graph \bar{G} is a spanning tree.

Assumption 2. Throughout the learning process, the initial and boundary conditions are consistently satisfied:

$$\sigma p_{j,k}(s, t) + \beta \frac{\partial p_{j,k}(s, t)}{\partial v} = 0, (s, t) \in \partial\Omega \times [0, T], \quad (4)$$

$$p_{j,k}(s, t) = \varphi_{j,k}(s), s \in \Omega, j \in \{1, 2, \dots, N\}, k \in Z^+, \quad (5)$$

where the function $\varphi_{j,k}(s)$ satisfies the following: $\|\varphi_{j,k+1}(s) - \varphi_{j,k}(s)\|_{L^2}^2 \leq l r^k, r \in [0, 1), l > 0$.

Remark 1. The mathematical symbols and lemmas in the Preliminaries lay the foundation for subsequent analysis and description. Based on references [13–17,36–39], the dynamic model is constructed in the problem statement, addressing the fault diagnosis problem for a class of partial differential MASs. Furthermore, appropriate ILC protocols are designed to diagnose faults within the MAS. To prove the convergence of this learning protocol, mathematical tools such as λ -norms, widely utilized in the convergence proof process, are employed, as seen in reference [36–39].

Remark 2. Assumption 1 ensures no isolated actuator agent is in MAS (1), guaranteeing the ability to estimate potential faults for each actuator agent. Assumption 2 serves as a fundamental condition in the design of the ILC, ensuring optimal tracking and estimation performance. This aligns with the approach taken in many ILC references [26–28], avoiding the sacrifice of tracking performance to eliminate this situation.

3. Design of Fault Estimation Tracker and Learning Control Protocol

To estimate the magnitude of fault when MAS (1) experiences a fault, and under the fulfillment of the aforementioned Assumptions 1–2, it is necessary to first design the following virtual fault tracking estimator:

$$\begin{cases} \frac{\partial \hat{p}_{j,k}(s,t)}{\partial t} = H\Delta \hat{p}_{j,k}(s,t) + A\hat{p}_{j,k}(s,t) + Bu_j(s,t) + E\hat{f}_{j,k}(s,t) + V(y_j(s,t) - \hat{y}_{j,k}(s,t)), \\ \hat{y}_{j,k}(s,t) = C\hat{p}_{j,k}(s,t) + Du_j(s,t) + F\hat{f}_{j,k}(s,t), \end{cases} \quad (6)$$

where k represents the iteration count, and $\hat{p}_{j,k}(s,t)$ and $\hat{y}_{j,k}(s,t)$ are the state and output estimation values of actuator agent j , respectively. For the sake of convenience, the corresponding symbols are denoted as follows:

$$\tilde{p}_{j,k}(s,t) = p_j(s,t) - \hat{p}_{j,k}(s,t), \quad (7)$$

$$\tilde{f}_{j,k}(s,t) = f_j(s,t) - \hat{f}_{j,k}(s,t), \quad (8)$$

$$e_{j,k}(s,t) = y_j(s,t) - \hat{y}_{j,k}(s,t), \quad (9)$$

where $\tilde{f}_{j,k}(s,t)$ represents the fault error of actuator agent j , while $e_{j,k}(s,t)$ corresponds to the difference between the output of actuator agent j and the output of the fault estimator (6), namely, the residual signal. $V \in R^{n \times p}$ is a predefined gain matrix.

To ensure that the virtual faults of the actuator agents approximate the actual faults through iteration, a P-type ILC protocol is designed based on the aforementioned residual signal $e_{j,k}(s,t)$, as follows:

$$\hat{f}_{j,k+1}(s,t) = \hat{f}_{j,k}(s,t) + \gamma \sum_{i=1}^N \bar{a}_{j,i} [(y_j(s,t) - \hat{y}_{j,k}(s,t)) - (y_i(s,t) - \hat{y}_{i,k}(s,t))], \quad (10)$$

where γ is the learning gain matrix. In the actual learning process, the correction of virtual faults by the fault estimator ceases when the actual output and estimator output of actuator agent j satisfy $\|y_j(s,t) - \hat{y}_{j,k}(s,t)\|_{L^2}^2 \leq \varepsilon$, where ε is a given performance metric. The correction of virtual faults stops when the estimate $\|y_j(s,t) - \hat{y}_{j,k}(s,t)\|_{L^2}^2 \leq \varepsilon$ is satisfied.

Inspired by references [15,26–28], the corresponding fault estimator and ILC protocol are designed. The core idea is as follows: within the selected optimization region, the residual signal is utilized between the actual output of actuator agent j in MAS (1) and the fault tracking estimation output. Further, the ILC protocol (10) is leveraged to adjust the introduced virtual faults. This adjustment is performed in such a way that the virtual faults gradually approach the true faults of actuator agent j in the MAS along the iteration axis. The ultimate goal is to achieve the estimation of this fault, i.e., $\lim_{k \rightarrow \infty} \|f_j(\cdot, t) - \hat{f}_{j,k}(\cdot, t)\|_{L^2}^2 = 0$. Simultaneously, this implies $\lim_{k \rightarrow \infty} \|y_j(\cdot, t) - \hat{y}_{j,k}(\cdot, t)\|_{L^2}^2 = 0$.

For the convenience of the subsequent convergence analysis of the fault estimator and control protocol, the corresponding compact forms are provided as follows:

$$\begin{cases} \frac{\partial \hat{p}_k(s,t)}{\partial t} = (I_N \otimes H)\Delta \hat{p}_k(s,t) + (I_N \otimes A)\hat{p}_k(s,t) + (I_N \otimes B)u(s,t) \\ \quad + (I_N \otimes E)\hat{f}_k(s,t) + (I_N \otimes V)(y(s,t) - \hat{y}_k(s,t)), \\ \hat{y}_k(s,t) = (I_N \otimes C)\hat{p}_k(s,t) + (I_N \otimes D)u(s,t) + (I_N \otimes F)\hat{f}_k(s,t), \end{cases} \quad (11)$$

where $\hat{p}_k(s,t) = [\hat{p}_{1,k}^T(s,t), \hat{p}_{2,k}^T(s,t), \dots, \hat{p}_{N,k}^T(s,t)]^T \in R^{Nn}$, $u(s,t) = [u_1^T(s,t), u_2^T(s,t), \dots, u_N^T(s,t)]^T \in R^{Nm}$, $y(s,t) = [y_1^T(s,t), y_2^T(s,t), \dots, y_N^T(s,t)] \in R^{Np}$, $\hat{y}(s,t) = [\hat{y}_{1,k}^T(s,t), \hat{y}_{2,k}^T(s,t), \dots, \hat{y}_{N,k}^T(s,t)] \in R^{Np}$,

$$\hat{f}(s, t) = [\hat{f}_{1,k}^T(s, t), \hat{f}_{2,k}^T(s, t), \dots, \hat{f}_{N,k}^T(s, t)] \in R^{Nm}.$$

$$\hat{f}_{k+1}(s, t) = \hat{f}_k(s, t) + (\bar{L} \otimes \gamma)e_k(s, t), \tag{12}$$

where $e_k(s, t) = y(s, t) - \hat{y}_k(s, t)$ represents the residual signal of the actuator agent in MAS (1), and $\bar{L} \in R^{N \times N}$ is the Laplacian matrix.

4. Convergence Analysis of Control Protocol

In order to ensure that the virtual fault estimator’s faults approximate the actual faults of the MAS through the previously designed ILC protocol, it is necessary to satisfy Theorem 1:

Theorem 1. *Under the Assumptions 1–2 for MASs (1) and utilizing the designed fault estimator, when estimating faults occurring in the system through the designed P-type iterative learning control (ILC) protocol, if the learning gain γ satisfies condition $\|I_N - (\bar{L} \otimes \gamma)(I_N \otimes F)\|_2 < 0.5$, accompanied by condition $k \rightarrow \infty$, then the faults of the virtual fault estimator approach the faults of the actual MASs (1), i.e., $\lim_{k \rightarrow \infty} \|f_j(\cdot, t) - \hat{f}_{j,k}(\cdot, t)\|_{L^2} = 0, j = 1, 2, \dots, N, t \in [0, T]$.*

Proof . From the above learning control protocol (12), the following is obtained:

$$f(s, t) - \hat{f}_{k+1}(s, t) = f(s, t) - \hat{f}_k(s, t) - (\bar{L} \otimes \gamma)e_k(s, t). \tag{13}$$

Then, Equations (7), (8) and (11), Equation (13) can be further expressed as follows:

$$\begin{aligned} \check{f}_{k+1}(s, t) &= \check{f}_k(s, t) - (\bar{L} \otimes \gamma)(I_N \otimes C)\check{p}_k(s, t) - (\bar{L} \otimes \gamma)(I_N \otimes F)f_k(s, t) \\ &= (I_N - (\bar{L} \otimes \gamma)(I_N \otimes F))f_k(s, t) - (\bar{L} \otimes \gamma)(I_N \otimes C)\check{p}_k(s, t) \\ &= (I_N - \gamma F_\otimes)f_k(s, t) - (\gamma C_\otimes)\check{p}_k(s, t), \end{aligned} \tag{14}$$

where $\gamma F_\otimes = (\bar{L} \otimes \gamma)(I_N \otimes F)$, $\gamma C_\otimes = (\bar{L} \otimes \gamma)(I_N \otimes C)$.

With Equations (8) and (11), through Equation (14), the following inequality holds:

$$\begin{aligned} \check{f}_{k+1}^T(s, t)\check{f}_{k+1}(s, t) &= \check{f}_k^T(s, t)(I_N - \gamma F_\otimes)^T(I_N - \gamma F_\otimes)\check{f}_k(s, t) - \check{f}_k^T(s, t)(I_N - \gamma F_\otimes)^T(\gamma C_\otimes)\check{p}_k(s, t) \\ &\quad - \check{p}_k^T(s, t)(\gamma C_\otimes)^T(I_N - \gamma F_\otimes)f_k(s, t) + \check{p}_k^T(s, t)(\gamma C_\otimes)^T(\gamma C_\otimes)\check{p}_k(s, t) \\ &\leq 2\check{f}_k^T(s, t)(I_N - \gamma F_\otimes)^T(I_N - \gamma F_\otimes)\check{f}_k(s, t) + 2\check{p}_k^T(s, t)(\gamma C_\otimes)^T(\gamma C_\otimes)\check{p}_k(s, t). \end{aligned} \tag{15}$$

Integrating the inequality (15) with respect to s over Ω , one obtains the following:

$$\begin{aligned} \left\| \check{f}_{k+1}(\cdot, t) \right\|_{L^2}^2 &\leq 2\mu \int_{\Omega} \check{f}_k^T(s, t)\check{f}_k(s, t)ds + 2\vartheta \int_{\Omega} \check{p}_k^T(s, t)\check{p}_k(s, t)ds \\ &\leq 2\mu \left\| \check{f}_k(\cdot, t) \right\|_{L^2}^2 + 2\vartheta \left\| \check{p}_k(\cdot, t) \right\|_{L^2}^2, \end{aligned} \tag{16}$$

where $\mu = \|I_N - (\bar{L} \otimes \gamma)(I_N \otimes F)\|_2^2$, $\vartheta = \|(\bar{L} \otimes \gamma)(I_N \otimes C)\|_2^2$.

Next, from Equations (1) and (11), we can obtain the following:

$$\begin{aligned} \frac{\partial p(s, t)}{\partial t} - \frac{\partial \hat{p}_k(s, t)}{\partial t} &= (I_N \otimes H)\Delta(p(s, t) - \hat{p}_k(s, t)) + (I_N \otimes A)(p(s, t) - \hat{p}_k(s, t)) \\ &\quad + (I_N \otimes E)(f(s, t) - \hat{f}_k(s, t)) + (I_N \otimes V)(y(s, t) - \hat{y}_k(s, t)). \end{aligned} \tag{17}$$

By rearranging Equation (17) using the indices from Equation (7), one can obtain the following:

$$\begin{aligned} \frac{\partial \widetilde{p}_k(s,t)}{\partial t} &= (I_N \otimes H)\Delta \widetilde{p}_k(s,t) + (I_N \otimes A)\widetilde{p}_k(s,t) + (I_N \otimes E)\widetilde{f}_k(s,t) \\ &\quad - (I_N \otimes V)(I_N \otimes C)\widetilde{p}_k(s,t) - (I_N \otimes V)(I_N \otimes F)\widetilde{f}_k(s,t) \\ &= (I_N \otimes H)\Delta \widetilde{p}_k(s,t) + [(I_N \otimes A) - (I_{NN} \otimes VC)]\widetilde{p}_k(s,t) + [(I_N \otimes E) - (I_{NN} \otimes VF)]\widetilde{f}_k(s,t) \\ &= (I_N \otimes H)\Delta \widetilde{p}_k(s,t) + A_\otimes \widetilde{p}_k(s,t) + E_\otimes \widetilde{f}_k(s,t), \end{aligned} \tag{18}$$

where $A_\otimes = (I_N \otimes A) - (I_{NN} \otimes VC)$, $E_\otimes = (I_N \otimes E) - (I_{NN} \otimes VF)$.

Multiplying both sides of Equation (18) by $\widetilde{p}_k^T(s,t)$, one can obtain the following:

$$\widetilde{p}_k^T(s,t) \frac{\partial \widetilde{p}_k(s,t)}{\partial t} = \widetilde{p}_k^T(s,t)(I_N \otimes H)\Delta \widetilde{p}_k(s,t) + \widetilde{p}_k^T(s,t)A_\otimes \widetilde{p}_k(s,t) + \widetilde{p}_k^T(s,t)E_\otimes \widetilde{f}_k(s,t). \tag{19}$$

Transposing Equation (18), multiplying both sides by $\widetilde{p}_k(s,t)$, and combining this with Equation (19), one obtains the following:

$$\begin{aligned} \frac{\partial (\widetilde{p}_k^T(s,t)\widetilde{p}_k(s,t))}{\partial t} &= 2\widetilde{p}_k^T(s,t)(I_N \otimes H)\Delta \widetilde{p}_k(s,t) + \widetilde{p}_k^T(s,t)(A_\otimes + A_\otimes^T)\widetilde{p}_k(s,t) + 2\widetilde{p}_k^T(s,t)E_\otimes \widetilde{f}_k(s,t). \end{aligned} \tag{20}$$

Integrating Equation (20) with respect to s over Ω yields, one obtains the following:

$$\begin{aligned} \frac{\partial (\|\widetilde{p}_k(\cdot,t)\|_{L^2}^2)}{\partial t} &= 2\int_\Omega \widetilde{p}_k^T(s,t)(I_N \otimes H)\Delta \widetilde{p}_k(s,t)ds + \int_\Omega \widetilde{p}_k^T(s,t)(A_\otimes + A_\otimes^T)\widetilde{p}_k(s,t)ds + 2\int_\Omega \widetilde{p}_k^T(s,t)E_\otimes \widetilde{f}_k(s,t)ds. \end{aligned} \tag{21}$$

Using Green’s formula, Equation (21) can be further written as follows:

$$\begin{aligned} \frac{\partial (\|\widetilde{p}_k(\cdot,t)\|_{L^2}^2)}{\partial t} &\leq 2\int_{\partial\Omega} \widetilde{p}_k^T(s,t)(I_N \otimes H) \frac{\partial \widetilde{p}_k(s,t)}{\partial \nu} ds - 2\int_\Omega \nabla \widetilde{p}_k^T(s,t)(I_N \otimes H)\Delta \widetilde{p}_k(s,t)ds \\ &\quad + \lambda_{\max}(A_\otimes + A_\otimes^T) \|\widetilde{p}_k(\cdot,t)\|_{L^2}^2 + \lambda_{\max}(E_\otimes) [\|\widetilde{p}_k(\cdot,t)\|_{L^2}^2 + \|\widetilde{f}_k(\cdot,t)\|_{L^2}^2]. \end{aligned} \tag{22}$$

From the MAS (1) boundary conditions, $\frac{\partial p(s,t)}{\partial \nu} = -\frac{1}{\beta}\sigma p(s,t)$ is held, and from inequality (22), one obtains the following:

$$\begin{aligned} \frac{\partial (\|\widetilde{p}_k(\cdot,t)\|_{L^2}^2)}{\partial t} &\leq 2\int_{\partial\Omega} \widetilde{p}_k^T(s,t)(I_N \otimes H) \left(-\frac{1}{\beta}\sigma\right) \widetilde{p}_k(s,t)ds + \lambda_{\max}(A_\otimes + A_\otimes^T) \|\widetilde{p}_k(\cdot,t)\|_{L^2}^2 \\ &\quad + \lambda_{\max}(E_\otimes) [\|\widetilde{p}_k(\cdot,t)\|_{L^2}^2 + \|\widetilde{f}_k(\cdot,t)\|_{L^2}^2] \leq \eta_1 \|\widetilde{p}_k(\cdot,t)\|_{L^2}^2 + \eta_2 \|\widetilde{f}_k(\cdot,t)\|_{L^2}^2, \end{aligned} \tag{23}$$

where $\eta_1 = \lambda_{\max}(A_\otimes + A_\otimes^T) + \lambda_{\max}(E_\otimes)$, $\eta_2 = \lambda_{\max}(E_\otimes)$.

Integrating both sides of inequality (23) with respect to t , and utilizing Lemma 2, one can obtain the following:

$$\begin{aligned} \|\widetilde{p}_k(\cdot,t)\|_{L^2}^2 &\leq \|\widetilde{p}_k(\cdot,0)\|_{L^2}^2 + \int_0^t (\eta_1 \|\widetilde{p}_k(\cdot,s)\|_{L^2}^2 + \eta_2 \|\widetilde{f}_k(\cdot,s)\|_{L^2}^2) ds \\ &\leq e^{\eta_1 t} \|\widetilde{p}_k(\cdot,0)\|_{L^2}^2 + \int_0^t \eta_2 e^{\eta_1(t-s)} \|\widetilde{f}_k(\cdot,s)\|_{L^2}^2 ds. \end{aligned} \tag{24}$$

By choosing $\lambda(\lambda > \eta_1)$ as appropriately large and multiplying both sides of the inequality (24) by $e^{-\lambda t}$, one obtains the following:

$$\|\widetilde{p}_k(\cdot,t)\|_{L^2}^2 e^{-\lambda t} \leq e^{\eta_1 t} \|\widetilde{p}_k(\cdot,0)\|_{L^2}^2 + \frac{\eta_2}{\lambda - \eta_1} \|\widetilde{f}_k\|_{(L^2,\lambda)}^2. \tag{25}$$

From the MAS (1) initial conditions, $\|\tilde{p}_k(\cdot, 0)\|_{L^2}^2 \leq lr^k$ is held. Therefore, inequality (25) can be further written as follows:

$$\|\tilde{p}_k(\cdot, t)\|_{L^2}^2 e^{-\lambda t} \leq lr^k + \frac{\eta_2}{\lambda - \eta_1} \|\tilde{f}_k\|_{(L^2, \lambda)}. \tag{26}$$

By multiplying both sides of the previous inequality (16) by $e^{-\lambda t}$ and substituting it into inequality (26), one obtains the following:

$$\begin{aligned} \|\tilde{f}_{k+1}(\cdot, t)\|_{L^2}^2 e^{-\lambda t} &\leq 2\mu \|\tilde{f}_k(\cdot, t)\|_{L^2}^2 e^{-\lambda t} + 2\vartheta \left\{ lr^k + \frac{\eta_2}{\lambda - \eta_1} \|\tilde{f}_k\|_{(L^2, \lambda)} \right\} \\ &\leq 2\vartheta lr^k + \left(2\mu + \frac{2\vartheta\eta_2}{\lambda - \eta_1} \right) \|\tilde{f}_k\|_{(L^2, \lambda)}, \end{aligned} \tag{27}$$

where $\rho = 2\mu + \frac{2\vartheta\eta_2}{\lambda - \eta_1}$. On one hand, since $0 \leq r < 1$, it implies that when $k \rightarrow \infty$, $r^k \rightarrow 0$. On the other hand, it is known that $2\mu < 1$. Based on the continuity of real numbers, it can be inferred that for a sufficiently large λ , $\rho < 1$ holds. Therefore, by Lemma 1, one can conclude the following:

$$\lim_{k \rightarrow \infty} \|\tilde{f}_k\|_{(L^2, \lambda)} = 0. \tag{28}$$

For $\forall t \in [0, T]$, one can obtain the following:

$$\|\tilde{f}_k(\cdot, t)\|_{L^2}^2 = \left(\|\tilde{f}_k(\cdot, t)\|_{L^2}^2 e^{-\lambda t} \right) e^{\lambda t} \leq \|\tilde{f}_k\|_{(L^2, \lambda)}^2 e^{-\lambda T}. \tag{29}$$

From Formulas (28) and (29), the following expression holds:

$$\lim_{k \rightarrow \infty} \|\tilde{f}_k(\cdot, t)\|_{L^2} = 0. \tag{30}$$

Since the aforementioned $\tilde{f}_k(\cdot, t)$ is the compact form of $\tilde{f}_{j,k}(\cdot, t)$, Equation (30) implies the following:

$$\lim_{k \rightarrow \infty} \|\tilde{f}_{j,k}(\cdot, t)\|_{L^2} = 0, j = 1, 2, \dots, N, t \in [0, T]. \tag{31}$$

In conclusion, it can be deduced that the L^2 norm of the fault regulation error of actuator agent j will gradually converge to zero along the iteration axis. The proof of Theorem 1 is completed. \square

In addition to Theorem 1, to ensure that the output of the virtual fault estimator approximates the system's actual output through the previously designed ILC protocol, it is necessary to satisfy Theorem 2.

Theorem 2. Under the same conditions as Theorem 1, the output of the fault estimator approximates the actual output, i.e., $\lim_{k \rightarrow \infty} \|y_j(\cdot, t) - \hat{y}_{j,k}(\cdot, t)\|_{L^2} = 0, j = 1, 2, \dots, N, t \in [0, T]$.

Proof . Next, to analyze the convergence of the output error, one can derive the following from Equation (9):

$$\begin{aligned}
 & e_k^T(s, t)e_k(s, t) \\
 &= \widetilde{f}_k^T(s, t)(I_N \otimes F)^T(I_N \otimes F)\widetilde{f}_k(s, t) + \widetilde{f}_k^T(s, t)(I_N \otimes F)^T(I_N \otimes C)\widetilde{p}_k(s, t) \\
 &\quad + \widetilde{p}_k^T(s, t)(I_N \otimes C)^T(I_N \otimes F)\widetilde{f}_k(s, t) + \widetilde{p}_k^T(s, t)(I_N \otimes C)^T(I_N \otimes C)\widetilde{p}_k(s, t) \\
 &\leq 2\lambda_{\max}[(I_N \otimes F)^T(I_N \otimes F)]\widetilde{f}_k^T(s, t)\widetilde{f}_k(s, t) + 2\lambda_{\max}[(I_N \otimes C)^T(I_N \otimes C)]\widetilde{p}_k^T(s, t)\widetilde{p}_k(s, t) \\
 &\leq 2\chi_1\widetilde{f}_k^T(s, t)\widetilde{f}_k(s, t) + 2\chi_2\widetilde{p}_k^T(s, t)\widetilde{p}_k(s, t),
 \end{aligned} \tag{32}$$

where $\chi_1 = \lambda_{\max}[(I_N \otimes F)^T(I_N \otimes F)]$, $\chi_2 = \lambda_{\max}[(I_N \otimes C)^T(I_N \otimes C)]$.

By integrating inequality (32) with respect to s over Ω , one can obtain the following:

$$\begin{aligned}
 \|e_k(\cdot, t)\|_{L^2}^2 &\leq 2\chi_1 \int_{\Omega} \widetilde{f}_k^T(s, t)\widetilde{f}_k(s, t)ds + 2\chi_2 \int_{\Omega} \widetilde{p}_k^T(s, t)\widetilde{p}_k(s, t)ds \\
 &\leq 2\chi_1 \left\| \widetilde{f}_k(\cdot, t) \right\|_{L^2}^2 + 2\chi_2 \left\| \widetilde{p}_k(\cdot, t) \right\|_{L^2}^2.
 \end{aligned} \tag{33}$$

By multiplying both sides of inequality (33) by $e^{-\lambda t}$, using inequality (26), one obtains the following:

$$\|e_k(\cdot, t)\|_{L^2}^2 e^{-\lambda t} \leq 2\chi_2 l r^k + \left(2\chi_1 + \frac{2\chi_2 \eta_2}{\lambda - \eta_1}\right) \left\| \widetilde{f}_k \right\|_{(L^2, \lambda)}. \tag{34}$$

Analysis reveals that both sides of inequality (34) are independent of time t . Therefore, the following inequality holds:

$$\|e_k\|_{(L^2, \lambda)} \leq 2\chi'_2 l r^k + \left(2\chi'_1 + \frac{2\chi'_2 \eta'_2}{\lambda - \eta'_1} + \frac{2\chi'_2 \eta'_2}{\lambda - \eta'_1}\right) \left\| \widetilde{f}_k \right\|_{(L^2, \lambda)}. \tag{35}$$

Similar to Formulas (27)–(31), one can obtain the following:

$$\lim_{k \rightarrow \infty} \left\| e_{j,k}(\cdot, t) \right\|_{L^2} = 0, j = 1, 2, \dots, N, t \in [0, T], \tag{36}$$

The proof of Theorem 2 is completed. □

5. Numerical Simulation

This section presents numerical simulations to demonstrate the effectiveness of the proposed fault diagnosis method. A class of partial differential MASs with actuators involving four actuator agents is considered, and the communication topology is shown in Figure 1.

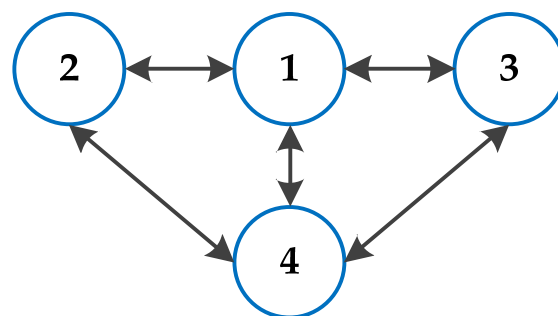


Figure 1. Connections between actuator agents.

Then, the corresponding Laplacian matrix of Figure 1 is as follows:

$$\bar{L} = \begin{bmatrix} 3 & -1 & -1 & -1 \\ -1 & 2 & 0 & -1 \\ -1 & 0 & 2 & -1 \\ -1 & -1 & -1 & 3 \end{bmatrix}.$$

The dynamic mathematical model and related parameters of the MASs are as follows:

$$\begin{cases} \frac{\partial p_j(s,t)}{\partial t} = H\Delta p_j(s,t) + Ap_j(s,t) + Bu_j(s,t) + Ef_j(s,t), \\ y_j(s,t) = Cp_j(s,t) + Du_j(s,t) + Ff_j(s,t), \end{cases} \quad (37)$$

where $j = 1, 2, 3, 4$ denotes the label of the actuator agent, and $(s, t) \in [0, 1] \times [0, 1]$, while $H = 1$. $A = \begin{bmatrix} 0.2 & 1.5 \\ 1 & -0.3 \end{bmatrix}$, $B = \begin{bmatrix} 0 & 0.1 \\ -0.5 & -0.6 \end{bmatrix}$, $E = \begin{bmatrix} -0.1 & 0 \\ 0 & -0.2 \end{bmatrix}$, $C = \begin{bmatrix} -0.3 & 0 \\ 0 & -0.2 \end{bmatrix}$, $D = \begin{bmatrix} 0.3 & 0 \\ 0 & 0.2 \end{bmatrix}$, $F = \begin{bmatrix} 0.3 & 0 \\ 0 & 0.2 \end{bmatrix}$. $V = \begin{bmatrix} 0.8 & 0 \\ 0 & 0.5 \end{bmatrix}$.

After selecting an appropriate learning gain, with the initial parameter set to $r = 0$, analysis and calculations reveal that these parameters satisfy the conditions of Theorems 1 and 2. Meanwhile, assuming the occurrence of fault in MAS (37), it is specified as follows:

$$f_j(s, t) = f_{j,d} = 6 \sin(12t) \sin(2s), j = 1, 2, 3, 4, \quad (38)$$

where $(s, t) \in [0, 1] \times [0, 1]$. Moreover, $j = 1, 2, 3, 4$ denotes the label of the actuator agent.

Utilizing the finite difference method for the differential equations and applying the previously designed fault estimator (11) and ILC protocol (12), the corresponding simulation results are illustrated in Figures 2–8.

Figure 1 depicts the connectivity among the actuator agents, noting that actuator agents 2 and 3 cannot directly exchange information. Figure 2 depicts the surface of the actual faults occurring in the actuator agents of MAS (37), while Figures 3 and 4 illustrate the surface of the faults in the estimator after 20 and 40 iterations of iterative learning, respectively. Combining Figures 2–4, it can be observed that the fault estimation in the estimator is approaching the actual output of the actuator agents.

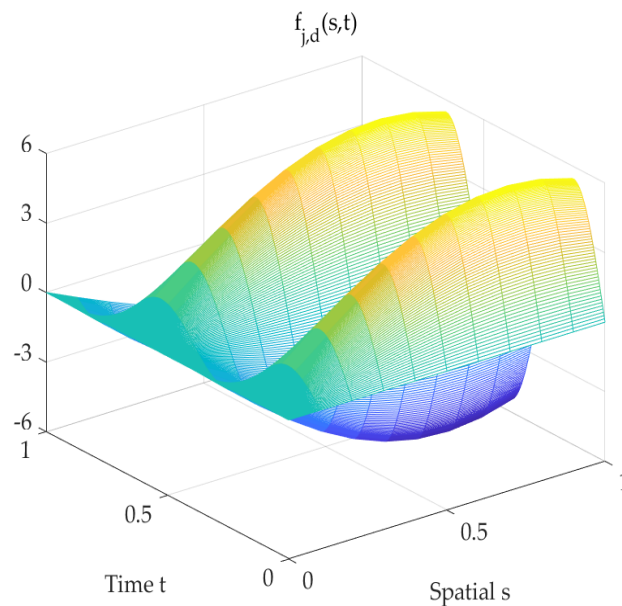


Figure 2. Actual fault $f_{j,d}(s, t)$ in actuator agent j of the systems (37).

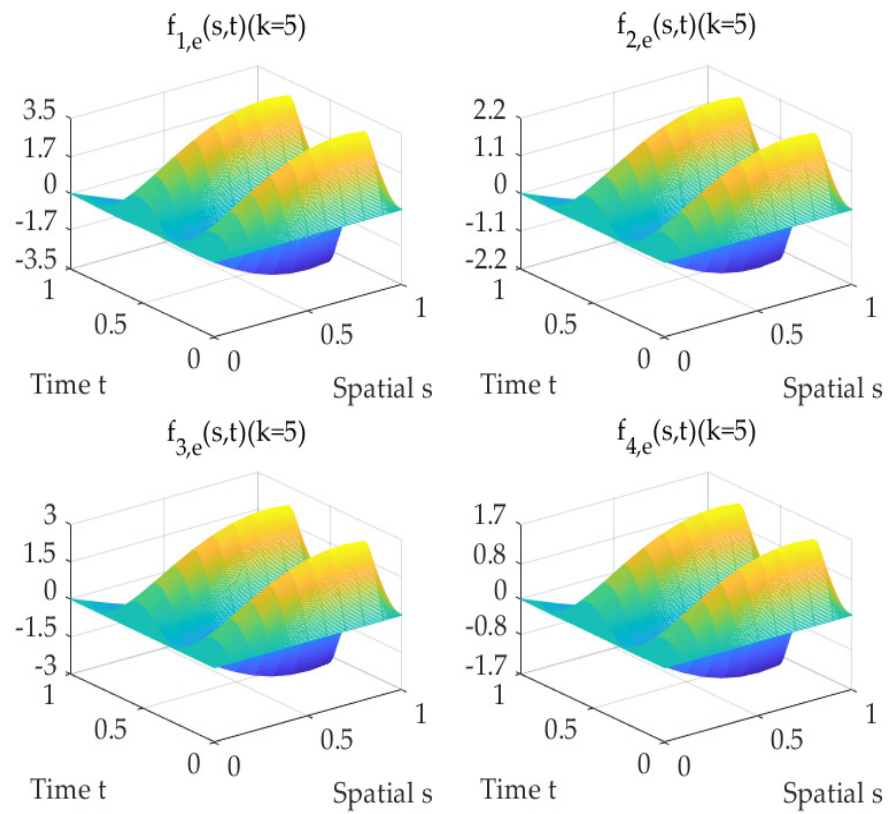


Figure 3. Fault estimation $f_{j,e}(s, t)$ ($k = 5$) in the estimator of the actuator agents.

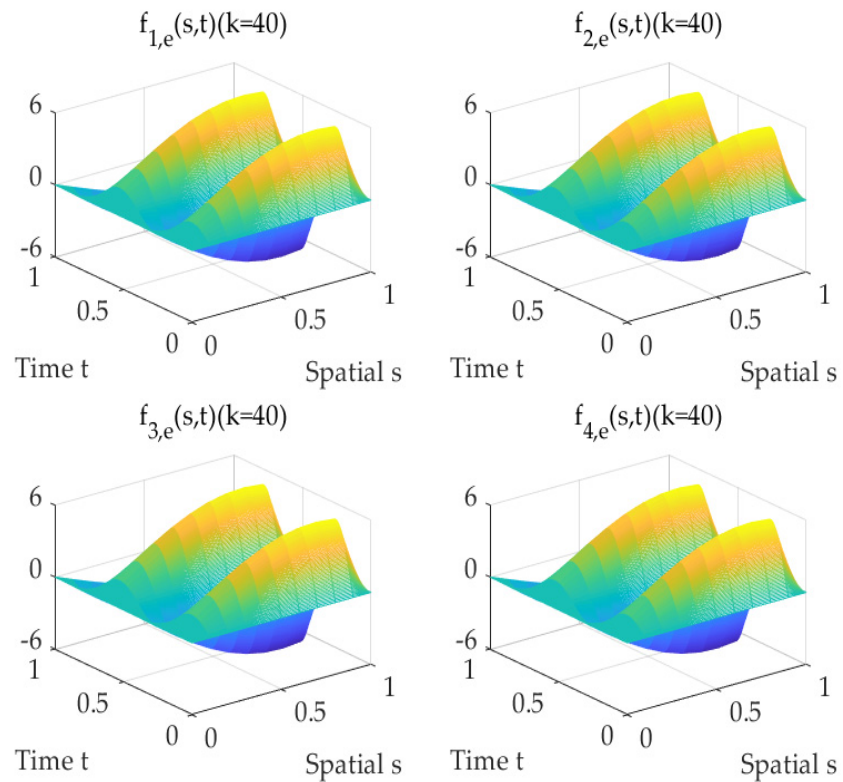


Figure 4. Fault estimation $f_{j,e}(s, t)$ ($k = 40$) in the estimator of the actuator agents.

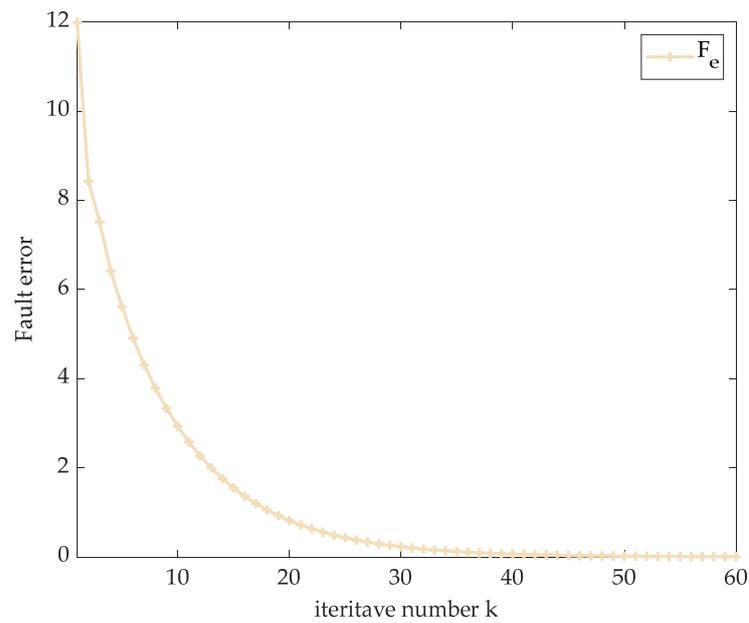


Figure 5. Fault error of system (37): iteration number curve.

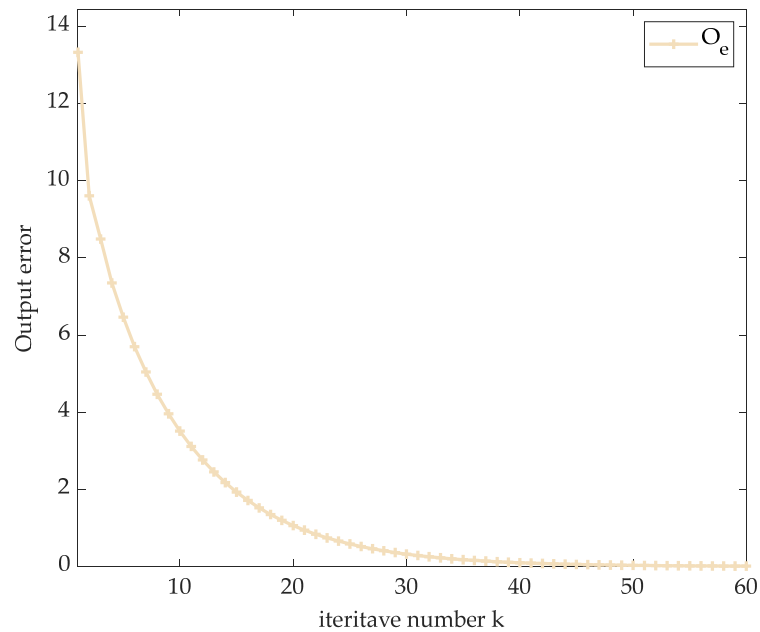


Figure 6. Output error of system (37); iteration number curve.

Figures 5 and 6 present curves depicting the variations in the fault error and output error in MAS (37) with the iteration count, respectively. Figures 7 and 8 present curves depicting the variations in the actuator fault error and output error with the iteration count, respectively. According to the varying curves in Figures 7 and 8, it can be observed that the fault errors and output errors of the four actuator agents gradually converge along the positive direction of the iteration axis. To further observe the variations in these errors, localized zoom-in plots are provided for each of them in Figures 7 and 8, respectively. By the 50th iteration, the fault errors and output errors of all actuator agents can enter the preset error band of 0.01. Therefore, Figures 7 and 8 show that with an increase in the number of iterative learning cycles, the fault estimation in the actuator agent’s estimator gradually converges to the actual fault, and the output also tends to approach the actual output.

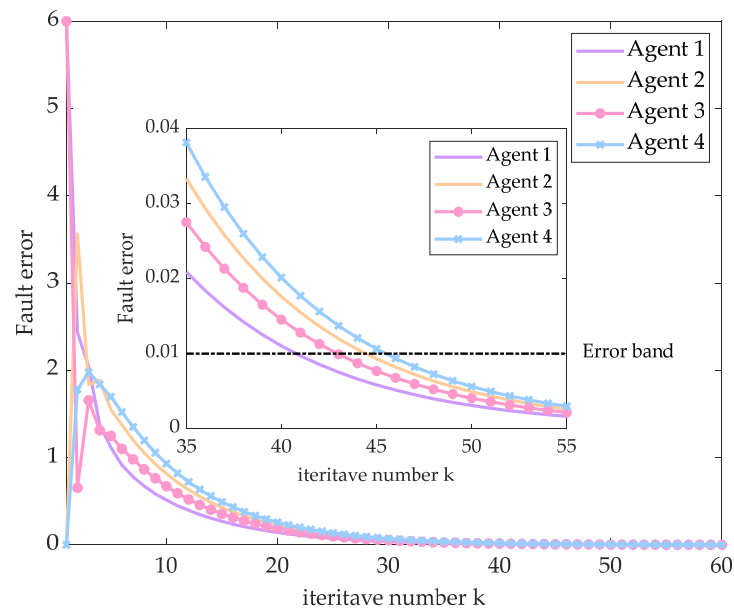


Figure 7. Fault error of actuator agents: iteration number curve.

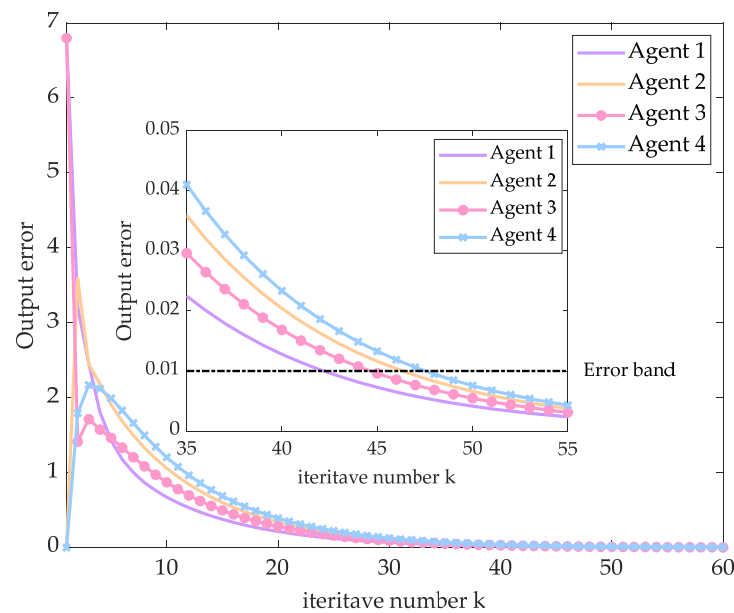


Figure 8. Output error of actuator agents: iteration number curve.

Figures 2–8 collectively demonstrate that the designed fault estimator can effectively track the partial differential MASs and learn and approximate faults.

6. Conclusions

This study investigates the fault diagnosis problem for parabolic partial differential MASs with actuators. A distributed virtual fault tracker and a p-type iterative learning fault-tracking protocol based on local measurement information among actuator agents are designed. A theoretical analysis of the learning protocol is rigorously conducted using contraction mapping and the Bellman–Gronwall lemma, providing convergence conditions for the protocol. The effectiveness of the proposed theory and learning protocol is validated through numerical simulation. However, it is worth noting that the study is limited to linear homogeneous MASs. Future research will address these limitations by considering more realistic nonlinear and heterogeneous MASs. Additionally, the applicability of this

protocol in fault diagnosis for multiple biomimetic robots and unmanned aerial vehicles will also be explored.

Author Contributions: Conceptualization, C.W. and J.W.; methodology, C.W. and J.W.; software, J.W.; validation, C.W. and Z.Z.; investigation, C.W., J.W. and Z.Z.; resources, J.W.; data curation, J.W.; writing—original draft preparation, C.W.; writing—review and editing, C.W., J.W. and Z.Z.; supervision, C.W. and J.W.; project administration, J.W. and Z.Z.; funding acquisition, C.W. and J.W. All authors have read and agreed to the published version of the manuscript.

Funding: This work is supported by Young and Middle-aged Teachers' Basic Scientific Research Ability Promotion Project in Guangxi Universities under Grant (No. 2021KY0852); Scientific Research Fund of Guangxi Science & Technology Normal University (GXKS2022ZD001); 2023 Demonstration modern Industry College construction project (GXKS2022ON006).

Data Availability Statement: The data presented in this study are available upon request from the corresponding author.

Conflicts of Interest: The authors declare no conflicts of interest.

References

- Liu, Y.; Jia, Y.M. An iterative learning approach to formation control of multi-agent systems. *Syst. Control Lett.* **2012**, *61*, 148–154. [[CrossRef](#)]
- Liu, X.C.; Chu, H.J.; Zhang, W.D. Observer-based adaptive consensus protocol design for multi-agent systems with one-sided lipschitz nonlinearity. *Mathematics* **2024**, *12*, 87. [[CrossRef](#)]
- Liu, D.Y.; Liu, H.; Liu, K.X.; Gu, H.B.; Lu, J.H. Robust hierarchical pinning control for nonlinear heterogeneous multiagent system with uncertainties and disturbances. *IEEE Trans. Circuits Syst. I* **2022**, *69*, 5273–5285. [[CrossRef](#)]
- Conte, G.; Scaradozzi, D.; Mannocchi, D.; Raspa, P.; Panebianco, L.; Screpanti, L. Development and experimental tests of a ros multi-agent structure for autonomous surface vehicles. *J. Intell. Robot. Syst.* **2018**, *92*, 705–718. [[CrossRef](#)]
- Pantelimon, G.; Tepe, K.; Carriveau, R.; Ahmed, S. Survey of multi-agent communication strategies for information exchange and mission control of drone deployments. *J. Intell. Robot. Syst.* **2019**, *95*, 779–788. [[CrossRef](#)]
- Liu, M. Applications of multi-agent systems. *Inf. Technol. Sel. Tutor.* **2004**, *157*, 239–270.
- Chen, Z.; Nian, X.H.; Meng, Q. Nash equilibrium seeking of general linear multi-agent systems in the cooperation-competition network. *Syst. Control Lett.* **2023**, *175*, 105510. [[CrossRef](#)]
- Zhou, Z.P.; Liu, X.F. State and fault estimation of sandwich systems with hysteresis. *Int. J. Robust. Nonlinear Control* **2018**, *28*, 3974–3986. [[CrossRef](#)]
- Zhou, Z.P.; Tan, Y.H.; Shi, P. Fault detection of a sandwich system with dead-zone based on robust observer. *Syst. Control Lett.* **2016**, *96*, 132–140. [[CrossRef](#)]
- Tchepemen, N.; Balasubramanian, S.; Kanagaraj, N.; Kengne, E. Modulational instability in a coupled nonlocal media with cubic, quintic and septimal nonlinearities. *Nonlinear Dyn.* **2023**, *111*, 20311–20329. [[CrossRef](#)]
- Cao, Y.Y.; Li, T.; Li, Y.; Wang, X.M. Heterogeneous multi-agent-based fault diagnosis scheme for actuation system. *Actuators* **2022**, *11*, 113. [[CrossRef](#)]
- Ye, Z.Y.; Jiang, B.; Cheng, Y.H.; Yu, Z.Q.; Yang, Y. Distributed fault diagnosis observer for multi-agent system against actuator and sensor faults. *J. Syst. Eng. Electron.* **2023**, *34*, 766–774. [[CrossRef](#)]
- Quan, Y.; Chen, W.; Wu, Z.H.; Peng, L. Distributed fault detection and isolation for leader-follower multi-agent systems with disturbances using observer techniques. *Nonlinear Dyn.* **2018**, *93*, 863–871. [[CrossRef](#)]
- Wang, Z.Y.; Li, S.H.; He, W.; Yang, R.H.; Feng, Z.C.; Sun, G.W. A new topology-switching strategy for fault diagnosis of multi-agent systems based on belief rule base. *Entropy* **2022**, *24*, 1591. [[CrossRef](#)]
- Chen, J.N.; Hua, C.C. Adaptive iterative learning fault-tolerant consensus control of multiagent systems under binary-valued communications. *IEEE Trans. Cybern.* **2023**, *53*, 6751–6760. [[CrossRef](#)]
- Natan, A.; Kalech, M.; Barták, R. Diagnosis of intermittent faults in multi-agent systems: An SFL approach. *Artif. Intell.* **2023**, *324*, 103994. [[CrossRef](#)]
- Zhong, Y.J.; Zhang, Y.M.; Ge, S.S.; He, X. Robust distributed sensor fault detection and diagnosis within formation control of multiagent systems. *IEEE Trans. Aerosp. Electron. Syst.* **2023**, *59*, 1340–1353. [[CrossRef](#)]
- Xu, J.X. Analysis of iterative learning control for a class of nonlinear discrete-time systems. *Automatica* **1997**, *33*, 1905–1907. [[CrossRef](#)]
- Arimoto, S.; Kawamura, S.; Miyazaki, F. Bettering operation of Robots by learning. *J. Robot. Syst.* **1984**, *1*, 123–140. [[CrossRef](#)]
- Bristow, D.A.; Tharayil, M.; Alleyne, A.G. A survey of iterative learning control. *IEEE Control Syst. Mag.* **2016**, *26*, 96–114.
- Rafajlowicz, W.; Jurewicz, P.; Reiner, J.; Rafajlowicz, E. Iterative learning of optimal control for nonlinear processes with applications to laser additive manufacturing. *IEEE Trans. Control Syst. Technol.* **2019**, *27*, 2647–2654. [[CrossRef](#)]

22. Luo, Z.J.; Xiong, W.J.; Huang, T.W.; Duan, J. Distributed quadratic optimization with terminal consensus iterative learning strategy. *Neurocomputing* **2023**, *528*, 12–19. [[CrossRef](#)]
23. Gu, P.P.; Wang, H.; Chen, L.P.; Chu, Z.B.; Tian, S.P. Iterative learning consensus control for one-sided lipschitz multi-agent systems. *Int. J. Robust Nonlinear Control* **2023**, *33*, 11257–11274. [[CrossRef](#)]
24. Xie, J.; Chen, J.X.; Li, J.M.; Chen, W.S.; Zhang, S. Consensus control for heterogeneous uncertain multi-agent systems with hybrid nonlinear dynamics via iterative learning algorithm. *Sci. China Technol. Sci.* **2023**, *66*, 2897–2906. [[CrossRef](#)]
25. Kuposov, A.S.; Pakshin, P.V. Iterative learning control of stochastic multi-agent systems with variable reference trajectory and topology. *Autom. Remote Control* **2023**, *84*, 612–625. [[CrossRef](#)]
26. Li, L.F.; Yao, L.N.; Wang, H.; Gao, Z.W. Iterative learning fault diagnosis and fault tolerant control for stochastic repetitive systems with Brownian motion. *ISA Trans.* **2022**, *121*, 171–179. [[CrossRef](#)]
27. Zhang, J.Y.; Huang, K. Fault diagnosis of coal-mine-gas charging sensor networks using iterative learning-control algorithm. *Phys. Commun.* **2020**, *43*, 101175. [[CrossRef](#)]
28. Patan, K.; Patan, M. Fault-tolerant design of non-linear iterative learning control using neural networks. *Eng. Appl. Artif. Intell.* **2023**, *124*, 106501. [[CrossRef](#)]
29. Zhou, X.Y.; Wang, H.P.; Tian, Y. Robust adaptive flexible prescribed performance tracking and vibration control for rigid-flexible coupled robotic systems with input quantization. *Nonlinear Dyn.* **2024**, *112*, 1951–1969. [[CrossRef](#)]
30. Stankovic, M.S.; Beko, M.; Stankovic, S.S. Distributed consensus-based multi-agent temporal-difference learning. *Automatica* **2023**, *151*, 110922. [[CrossRef](#)]
31. Najjar, A.; Karegar, H.K.; Esmailbeigi, S. Multi-agent protection scheme for microgrid using deep learning. *IET Renew. Power Gen.* **2024**, *18*, 663–678. [[CrossRef](#)]
32. Khatami, I.; Zahedi, M. Nonlinear vibration analysis of axially moving string. *SN Appl. Sci.* **2019**, *1*, 1668. [[CrossRef](#)]
33. Fan, X.; Xu, J.; Zhou, Q.; Leung, T. Dynamic modeling and control of flexible robotic manipulators. *Control Theory Appl.* **1997**, *14*, 318–335.
34. Song, X.N.; Zhang, Q.Y.; Wang, M.; Song, S. Distributed estimation for nonlinear PDE systems using space-sampling approach: Applications to high-speed aerospace vehicle. *Nonlinear Dyn.* **2021**, *106*, 3183–3198. [[CrossRef](#)]
35. Manikandan, K. Solitary wave solutions of the conformable space–time fractional coupled diffusion equation. *Partial Differ. Equ. Appl. Math.* **2024**, *9*, 100630. [[CrossRef](#)]
36. Dai, X.S.; Wang, C.; Tian, S.P.; Huang, Q.N. Consensus control via iterative learning for distributed parameter models multi-agent systems with time-delay. *J. Frankl. Inst.* **2019**, *356*, 5240–5259. [[CrossRef](#)]
37. Wu, J.; Dai, X.S.; Tian, S.P.; Huang, Q.N. Iterative learning consensus control of nonlinear impulsive distributed parameter multi-agent systems. *Eur. J. Control* **2023**, *71*, 100785. [[CrossRef](#)]
38. Zhou, M.; Wang, J.R.; Shen, D. Iterative learning based consensus control for distributed parameter type multi-agent differential inclusion systems. *Int. J. Robust Nonlinear Control* **2022**, *32*, 6785–6804. [[CrossRef](#)]
39. Wang, C.; Zhou, Z.P.; Dai, X.S.; Liu, X.F. Iterative learning approach for consensus tracking of partial difference multi-agent systems with control delay under switching topology. *ISA Trans.* **2023**, *136*, 46–60. [[CrossRef](#)]
40. Chen, Y.; Wen, C. *Iterative Learning Control: Convergence, Robustness and Applications*; Springer: London, UK, 1999; Volume 27.
41. Xie, S.; Chen, S. Stability criteria for parabolic type partial difference equations. *J. Comput. Appl. Math.* **1996**, *75*, 57–66. [[CrossRef](#)]

Disclaimer/Publisher’s Note: The statements, opinions and data contained in all publications are solely those of the individual author(s) and contributor(s) and not of MDPI and/or the editor(s). MDPI and/or the editor(s) disclaim responsibility for any injury to people or property resulting from any ideas, methods, instructions or products referred to in the content.